

$$b(\mu, \nu) = \frac{\zeta\phi + w(\phi)}{\zeta\nu + w(\nu)} \quad (74)$$

The function $w(x)$ is

$$w(x) = \int_{g(x)}^1 \frac{y}{f(y)} dy \quad (67)$$

The alternate expression for $w(x)$ is

$$w(x) = \int_0^x g(s) ds \quad (69)$$

The integrable first-order partial differential equation for ϕ is

$$\partial\phi/\partial\mu = -[\zeta\phi + w(\phi)] \quad (72)$$

The function $\phi(\mu, \nu)$ is the root of the function $G(x; \mu, \nu)$:

$$G(\phi; \mu, \nu) = 0 \quad (81)$$

where

$$G(x; \mu, \nu) = \ln \frac{\zeta x + w(x)}{\zeta \nu + w(\nu)} + H(x) - H(\nu) + (1 + \zeta)\mu \quad (82)$$

with derivative

$$\partial/\partial x G(x; \mu, \nu) = \frac{1 + \zeta}{\zeta x + w(x)} \quad (83)$$

The integral $H(x)$ used in the definition of G is

$$H(x) = \int_0^x \frac{1 - g(y)}{\zeta y + w(y)} dy \quad (77)$$

The quantum yield of the reaction of a sample with a thickness corresponding to a particular value of μ exposed to a dose of light ν is

$$\frac{Q}{Q_0} = (1 + \zeta) \frac{H(\nu) - H(\phi)}{\nu - \phi} \quad (90)$$

where

$$Q_0 = kF(C_r^0)/\Gamma_i^z$$

The contrast γ is

$$\gamma = -\nu \frac{g(\phi) - g(\nu)}{\zeta \nu + w(\nu)} \quad (96)$$

The dimensionless incident fluence is defined as

$$\nu_0(t) = \frac{kF(C_r^0)}{C_r^0} \int_{t_0}^t I_{\text{inc}}(t') dt' \quad (102)$$

The surface transmission coefficient is

$$S(\nu) = \frac{I_0(t)}{I_{\text{inc}}(t)} = \frac{d\nu(t)/dt}{d\nu_0(t)/dt} = S_f + (S_i - S_f)g(\nu) \quad (103)$$

or

$$S(\nu) = d\nu/d\nu_0 = S_f + (S_i - S_f)g(\nu) = S_f - \Delta S g(\nu) \quad (104)$$

where $\Delta S = S_f - S_i$. The equation relating ν_0 and ν is

$$S_f \nu_0 = \nu + K \left(\nu, \frac{\Delta S}{S_f} \right) \quad (107)$$

where

$$K(x, p) = p \int_0^x \frac{g(s)}{1 - pg(s)} ds \quad (108)$$

$$= p \int_{g(x)}^1 \frac{y}{(1 - py)f(y)} dy \quad (109)$$

The transmission coefficient of the entire sample is then

$$T(\mu, \nu_0) = \frac{I(z, t)}{I_{\text{inc}}(t)} = \frac{I(z, t)}{I_0(t)} \frac{I_0(t)}{I_{\text{inc}}(t)} = b(\mu, \nu) S(\nu) \quad (110)$$

where ν and ν_0 satisfy the relation given by eq 107.

Photolysis of Acetone at 193.3 nm

P. D. Lightfoot,[†] S. P. Kirwan, and M. J. Pilling*

Physical Chemistry Laboratory, South Parks Road, Oxford, U.K. (Received: October 28, 1987; In Final Form: February 23, 1988)

The photodecomposition of acetone by single-pulse excimer laser photolysis at 193 nm has been studied by using end product analysis and time-resolved absorption spectroscopy at 300 and 600 K and as a function of helium pressure. Ethane is the dominant product and the channel producing $2\text{CH}_3 + \text{CO}$ accounts for about 95% of the overall photolysis. It is suggested that the next most important channels produce $\text{H} + \text{CH}_2\text{COCH}_3$ (~3%) and $\text{CH}_4 + \text{CH}_2\text{CO}$ ($\leq 2\%$). Time-resolved experiments failed to detect acetyl radicals on a ~1-ms time scale, demonstrating that their yield is <1% of that of the methyl radical. The ethylene yield increases nonlinearly with laser energy, an observation attributed to secondary photolysis of vibrationally excited methyl radicals to yield $\text{CH}_2 + \text{H}$. The experiments demonstrate that 193-nm laser photolysis is a clean source of methyl radicals.

Introduction

The methyl radical plays an important role in a variety of high-temperature processes and a knowledge of its kinetics is necessary in the construction of numerical models. There is a need, therefore, for the determination of rate constants for methyl radical

reactions, preferably by time-resolved techniques using, for example, UV¹ or IR² absorption techniques and at high temperatures.

The flash photolysis of azomethane, using radiation in both the near-ultraviolet³ and far-ultraviolet,⁴ is known to provide a clean

(1) MacPherson, M. T.; Pilling, M. J.; Smith, M. J. C. *Chem. Phys. Lett.* **1983**, *94*, 430.

(2) Laguna, G. A.; Baughcum, S. L. *Chem. Phys. Lett.* **1982**, *88*, 568.

(3) Anastasi, C.; Maw, P. J. *Chem. Soc., Faraday Trans. 1* **1982**, *78*, 2423.

(4) Baggott, J. E.; Brouard, M.; Coles, M. A.; Davis, A.; Lightfoot, P. D.; MacPherson, M. T.; Pilling, M. J. *J. Phys. Chem.* **1987**, *91*, 317.

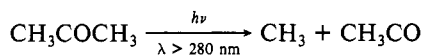
* Author to whom correspondence should be addressed.

[†] Present address: Laboratoire de Photophysique et Photochimie Moléculaire, UA CNRS No. 348, Université de Bordeaux, 33405 Talence Cedex, France.

source of methyl radicals and has been frequently employed; its low thermal stability, however, limits its use to temperatures below 600 K. Other possible sources such as acetaldehyde and the methyl halides suffer from potential complications caused by the unavoidable production of a second radical in the photolysis. This problem is particularly severe at the high (10^{13} – 10^{14} cm $^{-3}$) concentrations employed in studies using conventional optical absorption spectroscopy for radical detection.

The acetone molecule would appear to be a promising methyl radical source. It is thermally stable to well above 600 K on the time scale of typical flash photolysis experiments and absorbs UV radiation above its dissociation threshold in a region which is accessible using pulsed laser sources.

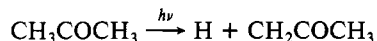
The photochemistry of the acetone molecule, excited via its first electronic absorption band ($\pi^* \leftarrow n_0$), which peaks at around 280 nm, has been much studied at wavelengths both above and below the dissociation limit.^{5–7} It is known that the predominant dissociation above 280 nm produces methyl and acetyl radicals:



Flash photolysis of acetone in this region has been used as a source of both methyl and acetyl radicals for kinetic measurements,⁸ but the presence of a second radical limits its usefulness as a methyl radical source. The acetyl radical yield decreases with increasing temperature, because of the increasing rate of thermal dissociation to CH_3 and CO ; reactions involving the acetyl radical were found to be insignificant above 423 K in end product analysis experiments employing low-intensity light sources with $\lambda > 280$ nm.^{9,10} The thermal dissociation of acetyl radicals could, however, complicate the methyl radical kinetics on the much shorter (microsecond to millisecond) time scale of flash photolysis/kinetic spectroscopy experiments.

The acetyl radical yield also decreases with decreasing wavelength below 280 nm, a consequence of either an increasingly rapid dissociation of the hot radicals produced in the initial photolysis step or the emergence of a second photolysis channel which directly produces two methyl radicals and carbon monoxide.

No evidence for the presence of stable acetyl radicals has been found in the photolysis of acetone excited via its second absorption band around 200 nm,^{11–13} although the single recent end product analysis study in this region employed a low-intensity light source, and the presence of short-lived acetyl radicals would not have been detected. The quantum yields for ethane and carbon monoxide were found to be around unity, with very small yields of minor products attributed to high-energy photolysis routes such as



Donaldson and Leone¹⁴ found prompt infrared emission from vibrationally excited CO on a microsecond time scale, following the 193.3-nm photolysis of acetone. The CO fragment rotation was, however, found to be very highly excited, suggesting that the fragmentation to produce two methyl radicals and carbon monoxide proceeded by a rapid two-step mechanism. However, Gandini and Hackett⁶ found that the quantum yield for carbon monoxide production in the region 255–280 nm was unaffected by the addition of several hundred Torr of an inert bath gas and

concluded that the direct route to carbon monoxide production was most likely, although they were not able to rule out the possibility of rapid predissociation from a low-lying excited electronic state of the acetyl radical. The available evidence thus suggests that the photolysis of acetone at around 200 nm, using a high-intensity, pulsed light source such as an exciplex laser at 193.3 nm (ArF), could provide a very clean source of methyl radicals for use in direct rate measurements. If a two-step mechanism pertains, then the acetyl radical is very short-lived. Furthermore, the extinction coefficient of acetone at 193.3 nm is around $700 \text{ M}^{-1} \text{ cm}^{-1}$,¹⁵ over a factor of 6 greater than the maximum of the first absorption band. The aim of the present work is to examine the products of the ArF exciplex laser photolysis of acetone and to establish its use as a clean methyl radical source for laser flash photolysis studies.

Experimental Section

Apparatus. The basis of the apparatus used in this study has been described previously.⁴ Gas mixtures, made up on an all-glass vacuum line, were transferred to a quartz cell (2.5 cm \times 9.7 cm) housed in a stainless steel heating block and were photolyzed by using defocused 193.3-nm radiation from an exciplex laser. After photolysis, the entire contents of the cell were transferred to a gas chromatograph for analysis. The transfer of gas mixtures between vacuum line, cell, and chromatograph was controlled by two six-port valves, one situated close to the cell and one located on the chromatograph.

The grease-free vacuum line was of conventional design and capable of achieving pressures of 1×10^{-5} Torr. Photolysis radiation was provided by an Oxford Lasers KX2 exciplex laser, operating on the ArF transition at 193.3 nm with a repetition rate of 0.5–1.0 Hz. Variation in the pulse energy, up to a maximum of 100 mJ, was achieved by inserting quartz flats in the beam path. The rectangular beam was defocused by using a 9 cm focal length biconvex quartz lens, so as to fill the body of the photolysis cell completely. The beam was checked regularly for homogeneity and adjusted if necessary.

A Varian Vista 44 system, incorporating both a flame ionization detector (used for hydrocarbon analysis) and a thermal conductivity detector (used for analysis of carbon monoxide), was employed for chromatographic analysis. A 4-m column of Chromosorb 102 (60/80 mesh), temperature programmed from 303 to 423 K, or, when analysis for carbon monoxide was required, from 263 to 423 K, was employed to separate the products.

The chromatograph was connected to the photolysis cell via two stainless steel, six-port valves (Valco), pneumatically driven by compressed nitrogen, the flow of which was controlled automatically from the chromatograph. Prior to analysis, the valves were configured so as to connect the cell to the vacuum line. After photolysis, the valves were switched, causing the contents to be pressurized by helium carrier gas and forced out to the chromatograph through a transfer line.

The all-quartz photolysis cell was of a construction, based on a design by Ledford and Braun,¹⁶ by which the carrier gas flowed into and out of the cell via annular end rings, ensuring >99% transfer of the cell contents (41.7 cm 3) in 8 min for a flow rate of 35 sccm. Despite the efficiency of the flushing system, it was necessary to retain the cell contents on a short liquid nitrogen-cooled precolumn for the transfer period. After transfer, the precolumn was allowed to warm up to the ambient oven temperature. This procedure effectively trapped the sample (including volatile components such as Ar and CO) on the first few column centimeters, resulting in sharp, well-resolved peaks.

Extensive calibrations for C1–C4 hydrocarbons and ketones showed that the transfer process was equally efficient for all molecules of interest. Responses were highly linear ($\pm 2\%$). Tests showed that a C3 hydrocarbon pressure in the cell as low as 2×10^{-6} Torr, corresponding to 2.6×10^{12} molecules cm $^{-3}$, could be detected and absolute hydrocarbon partial pressures of 10^{-4}

(5) Cundall, R. B.; Davies, A. S. *Prog. React. Kinet.* **1967**, *4*, 149 and references therein.

(6) Gandini, A.; Hackett, P. A. *J. Am. Chem. Soc.* **1977**, *99*, 6195.

(7) Greenblatt, G. D.; Ruhman, S.; Haas, Y. *Chem. Phys. Lett.* **1984**, *112*, 200.

(8) Adachi, H.; Basco, N.; James, D. G. L. *Chem. Phys. Lett.* **1978**, *59*, 502.

(9) Winkler, C. A. *Trans. Faraday Soc.* **1935**, *31*, 761.

(10) Herr, D. S.; Noyes, W. A., Jr. *J. Am. Chem. Soc.* **1940**, *62*, 2052.

(11) Manning, W. M. *J. Am. Chem. Soc.* **1934**, *56*, 2589.

(12) Howe, J. P.; Noyes, W. A., Jr. *J. Am. Chem. Soc.* **1936**, *58*, 1404.

(13) Potzinger, P.; Von Bunau, G. *Ber. Bunsen-Ges. Phys. Chem.* **1968**, *72*, 195.

(14) Donaldson, D. J.; Leone, S. R. *J. Chem. Phys.* **1986**, *85*, 817.

(15) Lake, J. S.; Harrison, A. J. *J. Chem. Phys.* **1959**, *30*, 361.

(16) Ledford, A. E.; Braun, W. *Rev. Sci. Instrum.* **1977**, *48*, 539.

TABLE I: Summary of Experimental Conditions

temp/ K	tot. press./ Torr	acetone press./ Torr	laser shots	photon density ^a / 10 ¹⁴ cm ⁻²	radical scavengers
300	500	0.53–2.56	10	11–29	NO, ^b C ₂ H ₄ ^c
	330	1.0	1–20	4–34	
	40	1.0	10	2–29	
	10	0.25	20	7–36	NO ^d
600	17.2	0.86	10	2–26	
	345	0.86	10	3–26	C ₂ H ₄ ^e

^a A 50-mJ pulse is equivalent to 1.8×10^{15} photons cm⁻² incident on the cell. ^b Laser pulse energy 80 ± 5 mJ, NO 0–2 Torr, acetone 1 Torr, 10 laser shots. ^c Laser pulse energy 80 ± 5 mJ, C₂H₄ 0–4 Torr, acetone 1 Torr, 10 laser shots. ^d Laser pulse energy 95 ± 6 mJ, NO 0–3 Torr, acetone 0.25 Torr, 20 laser shots. ^e Laser pulse energy 46 ± 8 mJ, C₂H₄ 0–1 Torr, acetone 0.86 Torr, 10 laser shots.

Torr or greater could be measured to better than $\pm 5\%$.

Chemicals. Acetone (BDH, Aristar, 99.8%) was degassed by extensive freeze–pump–thaw cycles. Detectable impurities were $1.3 \times 10^{-6}\%$ ethane, $5.0 \times 10^{-7}\%$ methyl ethyl ketone (MEK), and $7.0 \times 10^{-7}\%$ methane. Ethylene (Matheson, 99.7%) was thoroughly degassed and a small methane impurity removed by trap-to-trap distillation from 1-propanol/liquid nitrogen to liquid nitrogen. Traces of methane ($3.6 \times 10^{-6}\%$) remained. Nitric oxide (BDH, 99%) was rendered free from air and other nitrogen oxides by trap-to-trap distillation from isopentane/liquid nitrogen to liquid nitrogen until white in color. Helium (BOC, A grade) was supplied directly to the vacuum line through an Oxisorb filter to reduce oxygen to below 1 ppm.

Results

Experiments were performed at 300 and 600 K, and at total pressures of 10–500 Torr of He. Acetone partial pressures of around 1 Torr were employed, resulting in absorbances of ≈ 0.1 for a 2.5-cm path length. At each pressure and temperature, the effect of variation in the laser pulse energy, I , was examined.

In addition, the effect of the radical scavengers nitric oxide (for carbon-containing radicals) and ethylene (for hydrogen atoms) was investigated at fixed I . The experimental conditions employed are summarized in Table I.

All errors are quoted at the 95.45% confidence level.

Although the yields of the major photolysis products were sufficient to be readily detectable in single-shot experiments, multiple (typically 10) laser shots were required to produce reliably detectable quantities of minor products. None of the expected products have absorption coefficients which are significantly greater than that of the precursor at 193.3 nm and the fractional yields of all the observed products showed no systematic dependence on the number of laser shots: the observed products must thus arise from the photolysis of acetone alone.

Major Product Channel. Under all nonscavenged conditions, the major photolysis products were ethane, carbon monoxide, methane, and methyl ethyl ketone (MEK), in the approximate ratios 100:100:5:2.5. Much smaller quantities of ethylene, allene, propane, and (only at 600 K) propylene were found. Because of the large precursor:product concentration ratios (>20) employed, it was not possible to correlate precursor depletion with product formation accurately and thereby check for undetected photolysis routes.

The yield of ethane was independent of total pressure and scaled linearly with laser intensity, number of laser shots, and acetone partial pressure. Figure 1 shows a plot of the experimental ethane yield, corrected to 10 laser shots and 1 Torr of acetone, versus laser intensity, I , for all experiments at 300 K. Similar behavior was observed at 600 K, although the fractional decomposition of the precursor per laser shot was a factor of 1.9 greater than at 300 K for a given I , presumably because of an increase in the acetone extinction coefficient at 193.3 nm with temperature. The linear relationship between the ethane yield and I permits the former to be used as an internal monitor of intensity. The yield of ethane was independent of up to 10 Torr of added ethylene at

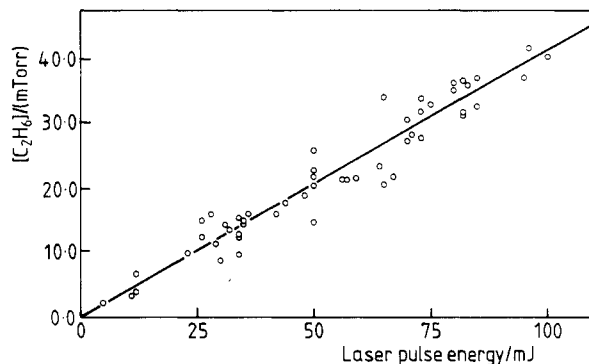


Figure 1. Ethane yield vs laser pulse energy, I , for all experiments at 300 K. The yields are scaled to refer to 10 laser shots and 1 Torr of acetone. The fitted straight line gives $F = (4.2 \pm 0.3) \times 10^{-5}I$, where F is the fractional photolysis of the precursor per laser shot and I is in mJ.

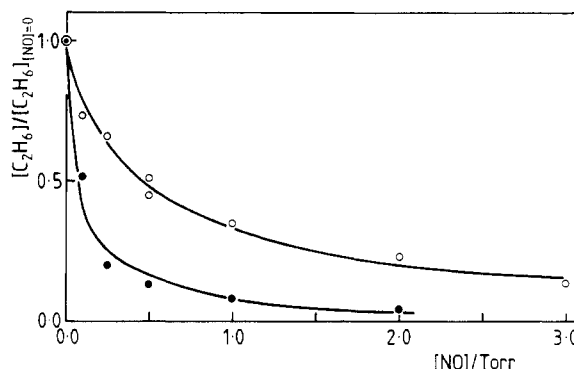
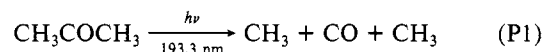


Figure 2. Dependence of ethane yield on NO partial pressure. Helium pressure: O, 10 Torr; ●, 500 Torr. Solid lines represent best fits to the data, assuming that methyl radicals are removed by recombination or reaction with NO, giving $k_6 = 4.2 \times 10^{-12}$ cm³ molecule⁻¹ s⁻¹ (500 Torr) and 6.9×10^{-13} cm³ molecule⁻¹ s⁻¹ (10 Torr).

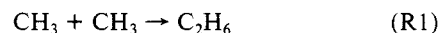
both temperatures but was very sensitive to the presence of nitric oxide, which reacts rapidly with methyl radicals to give a stable combination product. The dependence of the yield of ethane on [NO], relative to that found in the absence of the scavenger at 300 K and 10 and 500 Torr total pressure, is shown in Figure 2.

The yield of carbon monoxide was measured at room temperature and at 40, 330, and 500 Torr only. The ratio [CO]/[C₂H₆] was close to unity and independent of I in each case (Table II).

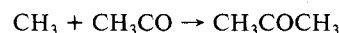
These results and the observed product ratios suggest that by far the most important photolysis channel at 193.3 nm is that producing methyl radicals and carbon monoxide



resulting in nearly equal yields of carbon monoxide and ethane, the latter being formed in the recombination reaction:



If a substantial fraction of the excited acetone molecules decomposed to give acetyl and methyl radicals, then a [C₂H₆]/[CO] ratio significantly greater than unity would be expected. However, small quantities of acetyl radicals would not be detected, as they would react with methyl radicals to regenerate the precursor:



A series of experiments was performed using laser flash photolysis/time-resolved UV absorption spectroscopy,¹⁷ in order to obtain more precise limits on the yield of acetyl radicals. The experiments were performed at 300 K and a total pressure of 330 Torr with 1 Torr of acetone. Similar laser fluences to those employed in the end product analysis experiments were used.

(17) Tulloch, J. M.; MacPherson, M. T.; Morgan, C. A.; Pilling, M. J. *J. Phys. Chem.* **1982**, *86*, 3812.

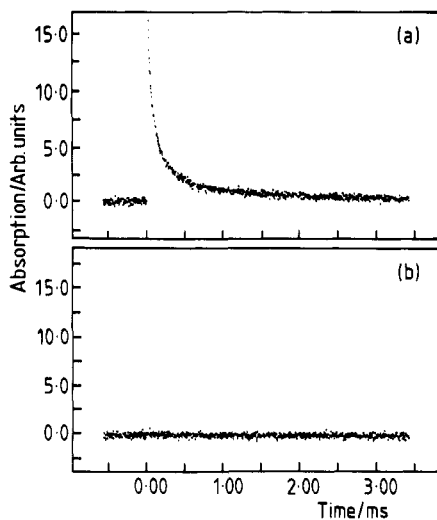


Figure 3. (a) Time-resolved absorption at 216.36 nm, following 193.3-nm photolysis. Nonlinear least-squares analysis of the second-order methyl radical decay gives $k_2/\sigma = 3.15 \times 10^6 \text{ cm s}^{-1}$. (b) Time-resolved absorption at 223 nm, following 193.3-nm photolysis of acetone.

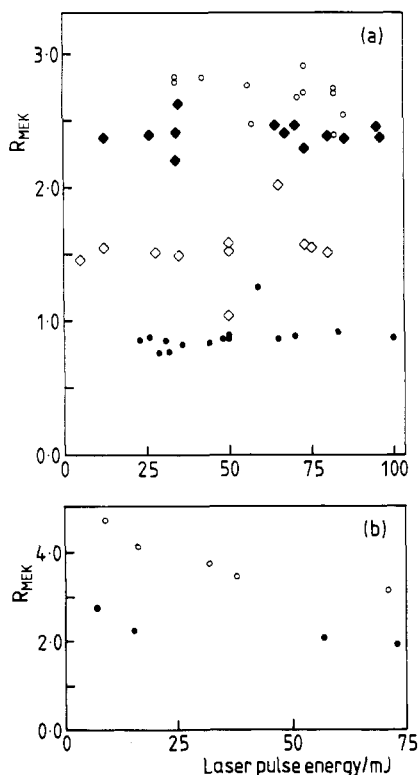


Figure 4. (a) Dependence of R_{MEK} on total pressure and laser pulse energy at 300 K. Helium pressure: ●, 10 Torr; ◇, 40 Torr; ◆, 330 Torr; ○, 500 Torr. (b) Dependence of R_{MEK} on total pressure and laser pulse energy at 600 K. Helium pressure: ●, 17.2 Torr; ○, 345 Torr.

Initially, the monochromator was set on the sharp methyl radical absorption at 216.36 nm, where $\sigma(\text{CH}_3) = 4.1 \times 10^{-17} \text{ cm}^2$ for a 0.6-nm band-pass.¹⁸ The resulting decays followed second-order kinetics, with $k_1/\sigma = 3.2 \times 10^6 \text{ cm s}^{-1}$, in good agreement with results obtained by using azomethane as the precursor;¹ Figure 3a shows a typical methyl radical decay profile. The UV photolysis of azomethane has been shown to provide a clean source of methyl radicals⁴ and has been used as such in several studies of methyl radical kinetics.^{1,18,19}

Subsequent attempts to detect acetyl radicals by absorption at 223 nm, where $\sigma(\text{CH}_3\text{CO}) = 1.0 \times 10^{-17} \text{ cm}^2$,²⁰ under identical

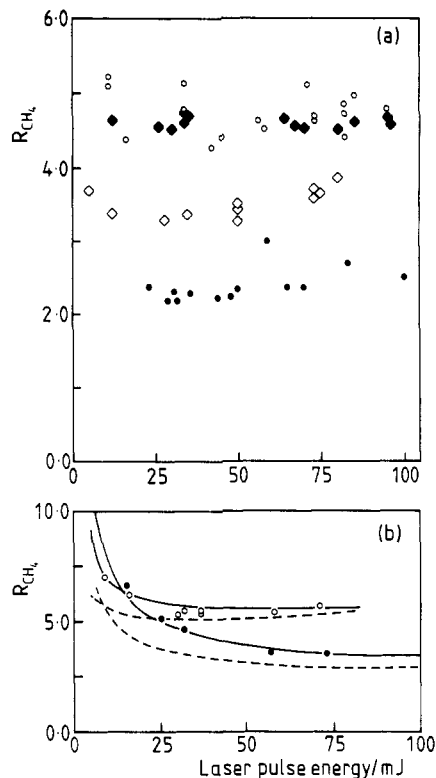


Figure 5. (a) Dependence of R_{CH_4} on total pressure and laser pulse energy at 300 K. Helium pressure: ●, 10 Torr; ◇, 40 Torr; ◆, 330 Torr; ○, 500 Torr. (b) Dependence of R_{CH_4} on total pressure and laser pulse energy at 600 K. Helium pressure: ●, 17.2 Torr; ○, 345 Torr. Bottom (dashed) curve of each pair: Rate constants taken from Table III. Top (full) curve: Rate constants as in Table III but with k_{10} increased by a factor of 2.

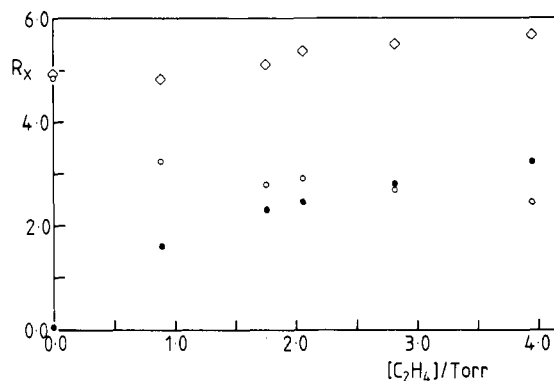


Figure 6. Dependence of product yields on $[\text{C}_2\text{H}_4]$, 300 K. Pressure 500 Torr of He, $I = 80 \text{ mJ}$. ●, $R_{\text{C}_3\text{H}_8}$; ○, R_{CH_4} ; ◇, $(R_{\text{C}_3\text{H}_8} + R_{\text{CH}_4})$.

experimental conditions, were unsuccessful. Any change in absorption after the laser pulse was well within the experimental noise, as shown in Figure 3b, enabling an upper limit of 0.01 to be placed on the ratio $[\text{CH}_3\text{CO}]/[\text{CH}_3]$ at $t = 0$.

Minor Product Channels. The dependences of the yields of the observed products on experimental conditions are summarized in Table II.

Methyl Ethyl Ketone. The yield of methyl ethyl ketone (MEK), relative to ethane, R_{MEK} (where $R_X = 100[X]/[\text{C}_2\text{H}_6]$), is shown as a function of pressure and laser intensity, I , at both experimental temperatures in Figure 4, a and b. R_{MEK} increased with pressure in each case. Although R_{MEK} was independent of I at 300 K, it decreased somewhat with increasing I at 600 K. Experimental averages of R_{MEK} at 300 K are given in Table II. MEK yields were unaffected by the presence of ethylene but were rapidly reduced to zero in the presence of nitric oxide.

(18) MacPherson, M. T.; Pilling, M. J.; Smith, M. J. C. *J. Phys. Chem.* **1985**, *89*, 2268.

(19) Pilling, M. J.; Smith, M. J. C. *J. Phys. Chem.* **1985**, *89*, 4713.

(20) Parkes, D. A. *Chem. Phys. Lett.* **1981**, *77*, 527.

TABLE II: Dependence of Product Yields on Experimental Conditions

	300 K				600 K		effect of NO	effect of C ₂ H ₄
	P ^a = 500	P = 330	P = 40	P = 10	P = 17.2	P = 345		
C ₂ H ₆		F ^b = (4.2 ± 0.3) ^c × 10 ⁻⁵ I ^d			F = (8.1 ± 1.3) × 10 ⁻⁵ I		reduced to zero	unaffected
R _{CO} ^e	100 ± 28	101 ± 26	129 ± 28	N/D ^f	N/D	N/D	N/D	N/D
R _{CH₄}	4.87 ± 0.80	4.43 ± 0.44	3.54 ± 0.38	2.29 ± 0.18	increased with decreasing I and increasing P		reduced	reduced
R _{MEK}	2.71 ± 0.44	2.43 ± 0.26	1.58 ± 0.58	0.82 ± 0.22	increased with decreasing I and increasing P		reduced to zero	unaffected
R _{C₃H₄}		0.17 ± 0.03			0.25 ± 0.10		N/D	unaffected
R _{C₃H₈}		0.09 ± 0.02			0.13 ± 0.08		N/D	increased
R _{C₂H₄}		(0.11 ± 0.06) + (2.6 ± 0.5) × 10 ⁻³ I			(0.16 ± 0.09) + (6.1 ± 2.1) × 10 ⁻³ I		reduced by ≈ 75%	N/D
R _{C₃H₆}		0.00			0.18 ± 0.12		N/D	N/D

^a Pressure, in Torr of He. ^b F is the fractional photolysis of the precursor per laser shot. ^c Errors 2σ. ^d Laser intensity I is in mJ. ^e R_x = 100[X]/[C₂H₆]. ^f Not determined.

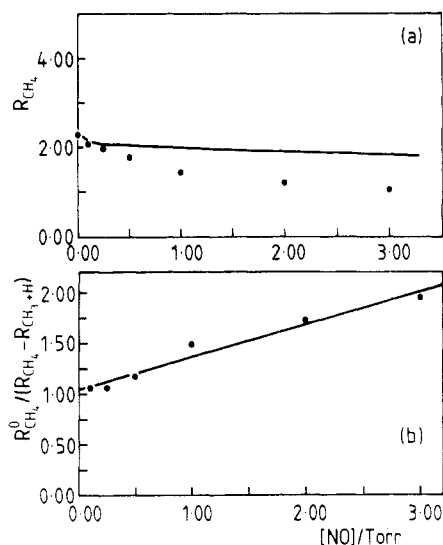


Figure 7. (a) Dependence of R_{CH_4} on [NO] at 300 K, 10 Torr of He. The solid line shows the simulated behavior, without allowance for electronic quenching. (b) Stern-Volmer plot for the quenching of the channel P3 by NO, 10 Torr total pressure. The straight line represents a best fit to the data.

Methane. The dependence of R_{CH_4} on I and pressure at 300 K is shown in Figure 5a and Table II. At this temperature, R_{CH_4} was independent of I , within experimental error, and increased with pressure. Addition of ethylene to photolysis mixtures resulted in a ≈ 50% reduction in the methane yield and a correspondingly large increase in the yield of propane, as shown in Figure 6.

Nitric oxide also reduced the yield of methane (Figure 7a), the effect being more pronounced at higher pressures.

R_{CH_4} was greater at 600 K than at room temperature and increased with decreasing I (Figure 5b). The addition of ethylene at this temperature caused R_{CH_4} to decrease rapidly up to 0.2 Torr of C₂H₄ and then more slowly with increasing [C₂H₄]. A correspondingly rapid initial rise in $R_{\text{C}_3\text{H}_8}$ was observed, followed by an apparently linear increase with [C₂H₄]. Although not found in the absence of ethylene, or in the 300 K experiments, minor quantities of *n*-butane, which increased linearly with [C₂H₄], and *n*-hexane were observed. The dependences of R_{CH_4} , $R_{\text{C}_3\text{H}_8}$, and $R_{\text{C}_2\text{H}_4}$ on [C₂H₄] at 600 K are shown in Figure 8.

Ethylene. Ethylene was observed as a minor product at both experimental temperatures. $R_{\text{C}_2\text{H}_4}$ was independent of total pressure and acetone partial pressure, but increased in an apparently linear fashion with I . Figure 9 shows the dependence of the absolute yield of ethylene, corrected to refer to 1 Torr of acetone and 10 laser shots, for all pressures at 300 K. $R_{\text{C}_2\text{H}_4}$ decreased rapidly with [NO], reaching a limiting value, corresponding to 25–30% of that found in the absence of the scavenger, at high nitric oxide concentrations.

C₃ Products. The only other products observed at both experimental temperatures were allene and propane. Both $R_{\text{C}_3\text{H}_4}$

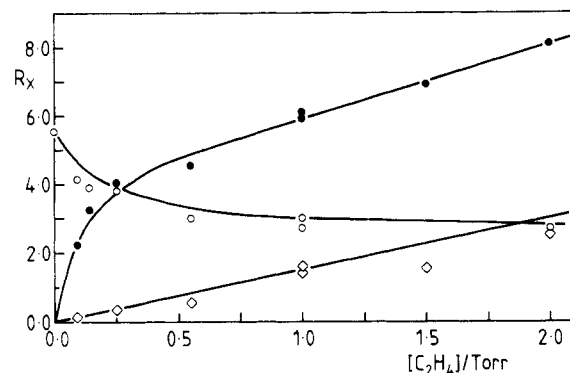


Figure 8. Dependence of product yields on [C₂H₄] at 600 K. Pressure = 345 Torr of He, $I = 46 \pm 8$ mJ. ○, R_{CH_4} ; ●, $R_{\text{C}_3\text{H}_8}$; ◇, $R_{\text{C}_2\text{H}_4}$. Solid lines show simulated dependences, after fitting to initial hydrogen atom and methane concentrations (see text).

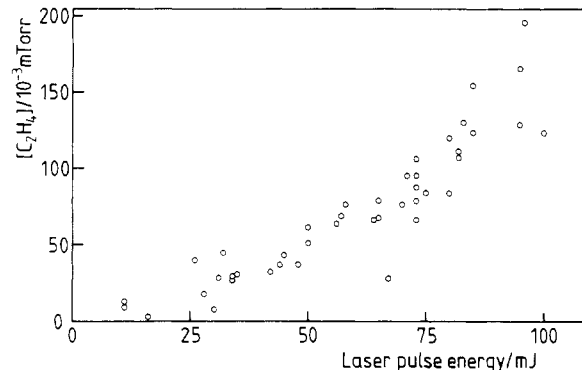


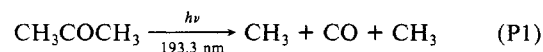
Figure 9. Dependence of the ethylene yield on laser pulse energy (300 K, all pressures). Yields are scaled to refer to 10 laser shots and 1 Torr of acetone.

and $R_{\text{C}_3\text{H}_8}$ displayed no significant dependence on total pressure, acetone partial pressure, or I and are given in Table II. It was not possible to determine the effect of nitric oxide on $R_{\text{C}_3\text{H}_4}$ and $R_{\text{C}_3\text{H}_8}$, as a GC base-line distortion occurred at their expected elution times, caused by the elution of a broad peak, which might be attributable to the products of the CH₃ + NO reaction. The presence of ethylene had no effect on $R_{\text{C}_3\text{H}_4}$; the dramatic increase in $R_{\text{C}_3\text{H}_8}$ with [C₂H₄] was discussed above.

Three additional minor products were found at 600 K, in yields similar to those of allene and propane and for which R_x was independent of I and total pressure. Unfortunately, only one of these additional products was identified as propylene.

Discussion

The present results clearly indicate that (P1) is the dominant photolytic process at 193.3 nm.



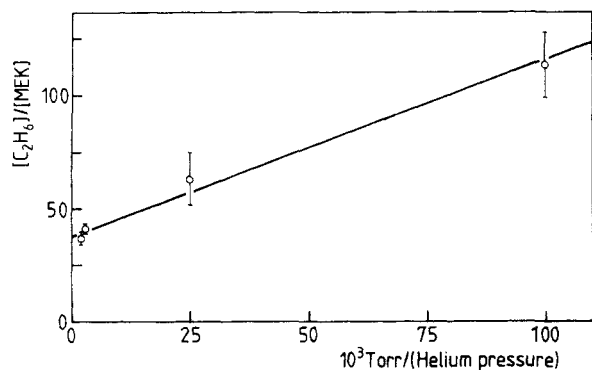


Figure 10. Plot of $1/R_{\text{MEK}}$ vs $1/\text{pressure}$ to determine R_{MEK}^0 , the limiting high-pressure value of the relative yield of methyl ethyl ketone.

The yields of hydrogen atoms R_{H} and nonscavengeable methane $R_{\text{CH}_4}^0$ were extracted from the observed values of R_{CH_4} and $R_{\text{C}_2\text{H}_6}$ by simulating the system by numerical integration of the differential equations determined by reactions R1–R5 (Table III), using the parameter-fitting facility of the numerical integration package FACSIMILE.²⁴ Initial concentrations were taken as

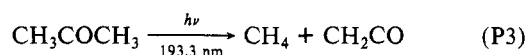
$$[\text{CH}_3]_{t=0} = 2.13 \times 10^{14} \text{ cm}^{-3}$$

$$[\text{H}]_{t=0} = [\text{C}_3\text{H}_8] + (1 - \beta)[\text{CH}_4]$$

$$[\text{CH}_4]_{t=0} = \beta[\text{CH}_4]$$

where β is the fraction of methane not produced via (R2). All end product concentrations were calculated per laser shot and corrected for dead volume. Values of β were obtained for each experiment. $R_{\text{CH}_4}^0 (= \beta R_{\text{CH}_4})$ displayed no systematic dependence on $[\text{C}_2\text{H}_4]$ and an average of six determinations gave $R_{\text{CH}_4}^0 = 1.60 \pm 0.18$.

Nonscavengeable methane has been observed in the 147-nm photolysis of acetone,²⁵ where it was attributed to a molecular elimination channel on the basis of isotopic labeling studies



and at 184.9 nm,¹⁸ where it was assumed to arise from abstraction reactions of vibrationally excited methyl radicals. In the present experiments, radical–bath gas collision rates were at least 3 orders of magnitude greater than the fastest radical–radical reaction rates and it is thus expected that radical–radical reaction involved encounters between thermalized radicals. It is known, however, that helium is a very inefficient collision partner for the relaxation of methyl radicals²⁶ and it is thus likely that collisions between vibrationally excited methyl radicals and precursor molecules occurred at all experimental pressures, although the hot radical reaction would have to be at least 3 orders of magnitude faster than the thermal reaction at 300 K²⁷ if significant quantities of methane were to be produced in this way. In addition, the ethylene scavenging experiments, from which $R_{\text{CH}_4}^0$ was determined, employed ethylene concentrations up to 4 times greater than the precursor concentration and no significant change in $R_{\text{CH}_4}^0$ with $[\text{C}_2\text{H}_4]$ was observed.

Sulfur hexafluoride is known to quench vibrationally excited methyl radicals very efficiently.²⁶ The addition of 10 Torr of SF_6 to a photolysis mixture of 1 Torr of acetone in 500 Torr of He produced no significant change in R_{CH_4} , demonstrating that, at least at the highest pressures used, hot methyl radical reactions were not important in the present experiments. The most probable route to nonscavengeable methane would, therefore, appear to be

(24) Chance, E. M.; Curtis, A. R.; Jones, I. P.; Kirby, C. R. FACSIMILE: A Computer Program for Flow and Chemistry Simulation, and General Initial Value Problems², AERE-R 8775; Atomic Energy Research Establishment: Harwell, U.K., 1977.

(25) Lin, L. J.-T.; Ausloos, P. J. *Photochem.* **1972**, *1*, 453.

(26) Callear, A. B.; Van Den Bergh, H. E. *Chem. Phys. Lett.* **1970**, *5*, 128.

(27) Ferguson, K. C.; Pearson, J. T. *Trans. Faraday Soc.* **1970**, *66*, 910.

(28) Brouard, M.; Pilling, M. J., to be submitted for publication.

TABLE IV: Comparison of Calculated and Experimental R_{CH_4} Values at 300 K

press./ Torr of He	exptl R_{CH_4}	simulated $R_{\text{CH}_4}^{a,b}$	
		with wall loss	without wall loss
500	4.87 ± 0.80	4.59	4.64
330	4.51 ± 0.44	4.51	4.63
40	3.54 ± 0.38	2.94	4.03
10	2.29 ± 0.18	1.85	2.77

^a $I = 45 \text{ mJ}$. ^b $R_{\text{CH}_4}^0 = 1.60$ added to calculated values of R_{CH_4} .

the molecular elimination channel P3.

A detailed analysis was made of the experiments conducted on the effects of C_2H_4 , NO, and pressure on the methane yield. Where necessary, comparisons were made with simulations. The main conclusions of this analysis are summarized as follows.

(i) Discrepancies between the molecular methane yields obtained from the ethylene and nitric oxide scavenging experiments can be attributed to quenching of the excited acetone precursor of channel P3 by NO. The data responded well to a Stern–Volmer treatment (Figure 7b), giving $k_q/k_d = (1.0 \pm 0.2) \times 10^{-17} \text{ cm}^3 \text{ molecule}^{-1}$, where k_q is the quenching rate constant and k_d the decay constant for the excited state of acetone. Thus, provided this quenching process is admitted, the effects on the methane yield of C_2H_4 , which scavenges H, and NO, which scavenges CH_3 , are compatible.

(ii) The yield of methane falls with pressure. This effect can be attributed to a competition between reaction R2, the rate of which decreases with pressure²⁹ and diffusion of H to the wall and its removal by a heterogeneous process. If it is assumed that H is removed with unit efficiency at the wall, then the calculated rate constant for wall removal becomes comparable to reaction with $[\text{CH}_3]_{t=0}$ at a pressure of ≈ 20 Torr; i.e., heterogeneous loss provides a feasible mechanism to explain the reduction in methane yield with decreasing pressure. These qualitative conclusions were confirmed by detailed simulations (vide infra).

(iii) Simulations based on the mechanism given in Table III demonstrate that acetyl radicals are not exclusively removed by (R3), as was assumed above in deducing the yield of (P2). Instead, a small but significant fraction ($\approx 13\%$) reacts via (R9). Correcting for this recombination process increases R_{MEK}^0 to (3.1 ± 0.6) .

As a final check on the validity of the yields of channels P2 and P3, Table IV compares the experimental and simulated methane yields. The simulations were performed with and without a heterogeneous loss process, whose rate constant was calculated assuming unit efficiency of wall removal. The agreement is satisfactory, suggesting, perhaps, that wall loss occurs with an efficiency of ≈ 0.5 . The reduction in the yield of methane found in the simulations which did not include the wall loss term arises, once again, from the decrease in k_2 with decreasing pressure. In this case, the H atoms are left unreacted when CH_3 recombination is complete and react at longer times, e.g., to generate H_2 .

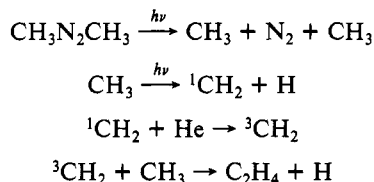
(P4) and (S1). The relative yield of the minor product ethylene was independent of pressure and acetone concentration but dependent on laser energy, unlike all other product yields. $R_{\text{C}_2\text{H}_4}$ increased from ≈ 0.2 at 25 mJ pulse⁻¹ to ≈ 0.35 at 80 mJ pulse⁻¹.

A nonlinear dependence of a product on I can arise in two ways. Firstly, if the product was formed in a process which was second-order in overall radical concentration and which was in competition with a first-order process, then the relative yield of the second-order process would increase with I . The identical dependences of the scaled yields of ethylene on I at 10 Torr, where the acetone partial pressure was 0.25 Torr and at other pressures where 1 Torr of the precursor was used and initial radical concentrations were a factor of 4 higher for a given I , show that such a mechanism is not operating in the present experiments (the reactions of hydrogen atoms²⁹ and methyl radicals²⁷ with acetone

(29) Kerr, J. A. In *Comprehensive Chemical Kinetics*; Bamford, G. H., Tipper, C. F. H., Eds.; Elsevier: New York, 1976.

are negligibly slow at 300 K under the present experimental conditions).

A second possibility is that ethylene arises from a multiphoton process. Given that the laser light was defocused into the cell, resulting in photon densities of $\approx 1 \times 10^{15} \text{ cm}^{-2}$ or power densities of $\approx 0.1 \text{ MW cm}^{-2}$ in a 10-ns pulse, it is unlikely that a coherent multiphoton process is occurring to a measurable extent and the sequential absorption of further 193.3-nm photons by a real excited state or a photolysis product is much more probable. Ethylene has been observed at high intensities in both the 193.3-nm⁴ and broad-band flash lamp photolysis³⁰ of azomethane. It was suggested that the mechanism of ethylene production involved the absorption of a second photon by methyl radicals generated in the initial part of the photolysis pulse, producing singlet methylene, which was rapidly quenched by the buffer gas to the triplet ground state,³¹ which in turn reacted with methyl radicals to generate ethylene and hydrogen atoms.



The ground-state methyl radical displays a strongly predissociated absorption band at 216.36 nm, assigned to the (0-0) transition of the $\tilde{\text{B}}^2\text{A}_1' \leftarrow \tilde{\text{X}}^2\text{A}_2''$ band.³³ The transitions with $\Delta v = 0$ will move to shorter wavelengths with increasing vibrational excitation, because of the large increase in the frequency of the ν_2 mode on promotion from the $\tilde{\text{X}}$ (606 cm^{-1}) to the $\tilde{\text{B}}$ (1360 cm^{-1}) state. Thus highly vibrationally excited methyl radicals might be expected to absorb at 193.3 nm.

Vibrationally excited methyl radicals have been observed in the photolysis of azomethane at 193.3 nm,¹⁸ the flash lamp photolysis of dimethylmercury,²⁶ and the photodissociation of methyl iodide at 266 nm.³³ In the latter case, a population inversion in the ν_2 mode was observed. Excitation of the methyl radical out-of-plane bending mode is likely to occur in all photodissociations producing methyl radicals, because of the change in methyl radical geometry from a tetrahedral to a planar configuration. In consequence, this mechanism of methylene production could be generally applicable to pulsed laser photolysis around 200 nm.

Support for this mechanism of ethylene production is found in the observation that much greater ethylene yields were found in the flash lamp photolysis of azomethane³⁰ than in the corresponding ArF excimer photolysis.⁴ The much broader spectral range generated by flash lamps would result in the possibility of absorption of further photons by methyl radicals from a wide range of vibrational levels in the electronic ground state.

Further evidence for the presence of methylene in the 193.3-nm photolysis of acetone at high intensities is provided by the work of Nagata et al.,³⁴ who monitored $\tilde{\text{A}}^2\Delta \rightarrow \tilde{\text{X}}^2\Sigma$ emission from electronically excited CH radicals, produced by a three-photon process in the photolysis of several methyl radical precursors, including acetone, using focused 193.3-nm radiation. The CH $\tilde{\text{A}}$ state rotational distributions were found to be bimodal and

virtually independent of precursor; it was concluded that $\text{CH } \tilde{\text{A}}^2\Delta$ radicals were produced by two mechanisms, both of which involved absorption of a second photon by methyl radicals produced in the initial photolysis step.

In order to increase the range of intensities covered in the present experiments, an experiment was performed at 330 Torr of He and a laser pulse energy of 85 mJ, but without the defocusing lens in place. It is estimated that the laser intensity in the rectangular irradiated section of the cell body was increased by approximately a factor of 11 in this way. $R_{\text{C}_2\text{H}_4}$ increased by a factor of 13, providing strong evidence for the existence of a two-photon mechanism for ethylene production. Furthermore, R_{CH_4} was also increased, from 4.4 to 13.9, demonstrating a significant increase in the yield of hydrogen atoms. The above mechanism predicts that two hydrogen atoms would be produced for each ethylene molecule observed. Assuming that all the hydrogen atoms react with methyl radicals to form methane, then the increase in R_{CH_4} should be equal to twice the increase in $R_{\text{C}_2\text{H}_4}$, in approximate agreement with the experimental results.

It must be emphasized that methylene constitutes only a very minor fraction of the radical products at the low intensities employed in the main experiments reported here and will not effect the suitability of acetone as a methyl radical source in flash photolysis/kinetic spectroscopy experiments.

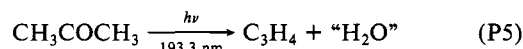
If all the observed ethylene were produced by the two-photon mechanism, then the addition of nitric oxide would be expected to reduce its yield rapidly to zero. A decrease in $[\text{C}_2\text{H}_4]$ with $[\text{NO}]$ was indeed observed, but the ethylene yield did not go to zero at high $[\text{NO}]$ and appeared to reach a stationary value at both 10 and 500 Torr corresponding to 25–30% of the value obtained in the absence of NO. Nonscavengable ethylene was observed in the 147-nm photolysis²⁵ of acetone, where isotopic studies showed that it arose from molecular elimination. A mechanism involving 1,1 elimination of a hydrogen molecule, followed by rapid rearrangement and dissociation of the carbene so formed, was proposed:



Given the scatter in the present ethylene yields, it is possible that some of the ethylene was produced by such a single-photon process. If both one- and two-photon processes were occurring, then $R_{\text{C}_2\text{H}_4}$ would be expected to vary linearly with I , but with a nonzero intercept. A linear fit to $R_{\text{C}_2\text{H}_4}$ vs I for the unscavenged experiments gave $R_{\text{C}_2\text{H}_4} = (0.11 \pm 0.06) + (2.6 \pm 0.5) \times 10^{-3} I/\text{mJ}$, where the gradient and intercept refer to the yields of ethylene produced via the two- and one-photon processes, respectively. From this fit, the yield of molecular ethylene is calculated to be 32% of the total at $I = 90 \text{ mJ}$, close to the value observed in the NO scavenging experiments.

It is expected that the hydrogen atoms produced via the photolysis of methyl radicals will contribute to the observed methane yield at high pressures where diffusion of the walls of the cell is not the dominant pathway for hydrogen atom removal and result in an increase in R_{CH_4} with I . However, the increase in the hydrogen atom yield R_{H} and hence in R_{CH_4} is calculated to be 0.42 over the range 10–90 mJ, which is well within the 95% confidence limits on R_{CH_4} at the two highest pressures.

Other Channels. Both allene (1.5%) and propane (0.3%) have been observed in the 147-nm photolysis of acetone. Nitric oxide scavenging experiments at that wavelength showed that, although propane was formed via a radical mechanism, allene was a primary photolysis product, and that methyl acetylene was produced in similar yields. In the present experiments, methylacetylene could not be separated from acetone.



The mechanism by which allene is produced is not obvious, although direct elimination of a water molecule would appear to be highly improbable and a stepwise fragmentation much more likely. One possible pathway could involve the cleavage of the

(30) Pilling, M. J.; Robertson, J. A.; Rogers, G. J. *Int. J. Chem. Kinet.* **1976**, *8*, 883.

(31) Ashfold, M. N. R.; Fullstone, M. A.; Hancock, G.; Ketley, G. W. *Chem. Phys.* **1981**, *55*, 245.

(32) Herzberg, G. *Electronic Spectra of Polyatomic Molecules*; Van Nostrand: New York, 1966.

(33) Sparks, R. K.; Shobotake, K.; Carlson, L. R.; Lee, Y. T. *J. Chem. Phys.* **1981**, *75*, 3838.

(34) Nagata, T.; Suzuki, M.; Suzuki, T.; Kankaru, T.; Kondow, T. *Chem. Phys.* **1984**, *88*, 163.

(35) Slagle, I. R.; Gutman, D.; Davies, J. W.; Pilling, M. J. *J. Phys. Chem.* **1988**, *92*, 2455.

(36) Lightfoot, P. D.; Pilling, M. J. *J. Phys. Chem.* **1987**, *91*, 3373.

(37) Davies, J. W.; Pilling, M. J., unpublished work.

(38) Ahumada, J. J.; Michael, J. V.; Osborne, D. T. *J. Chem. Phys.* **1972**, *57*, 3736.

(39) Adachi, H.; Basco, N. *Int. J. Chem. Kinet.* **1981**, *13*, 367.

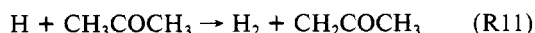
(40) Allara, D. L.; Shaw, R. *J. Phys. Chem. Ref. Data* **1980**, *9*, 523.

carbon-oxygen bond, followed by the elimination of molecular hydrogen from the dimethylcarbene so formed, to produce allene and methyl acetylene.

The origin of propane in the present system is even less clear, but given the extremely low yields of both allene and propane, the mechanisms by which they are produced are not of great significance; of greater significance, perhaps, is the demonstration, provided by the detection of such small product yields, of the sensitivity of the sampling technique.

Photolysis Yields at 600 K. With the exception of three very minor products, the end products seen in nonscavenging experiments at 600 K were identical with those observed at room temperature; the photolysis scheme developed to account for the 300 K products should be largely applicable to experiments at the higher temperature.

The chief differences between the observed behavior at 300 and 600 K were found in the values of R_{CH_4} and R_{MEK} obtained. Both R_{CH_4} and R_{MEK} increased with temperature and displayed a dependence on I at 600 K, but not at 300 K. These differences can be attributed to the radical-molecule reactions



which, although slow at room temperature, have large temperature coefficients and contribute significantly to the overall kinetics at 600 K. Pseudo-first-order loss rates for the removal of methyl radicals via (R10) and hydrogen atoms via (R11) are calculated, at 600 K, to be 2.3 and 955 s^{-1} , respectively, for an acetone partial pressure of 0.86 Torr. Although removal of methyl radicals by reaction with the precursor would still be very slow compared with removal by recombination at short times after the laser pulse, (R10) would become more important at long times and at low intensities. Similarly, (R11) would be expected to be most important at low intensities.

The presence of small quantities of *n*-butane and *n*-hexane in the scavenging experiments indicated that the addition of methyl radicals to ethylene was not negligible at 600 K and that reactions involving the *n*-propyl radical would have to be included in the reaction scheme used to model such experiments. Figure 8 shows a comparison of experimental and simulated product yields. For each scavenging experiment, best fit initial concentrations of hydrogen atoms and methyl radicals were obtained from the observed yields of ethane, methane, and propane, by numerical integration of the reaction scheme (R1)–(15). The fitted initial hydrogen atom concentrations were linear in $[\text{C}_2\text{H}_4]$, with an intercept corresponding to the yield of hydrogen atoms in the absence of ethylene, giving $R_{\text{H}} = 4.18 \pm 0.24$. The linear increase in R_{H} with ethylene concentration is caused by the photolysis of the scavenger. Although very little photolysis of ethylene was noticed at 300 K, its extinction coefficient at 193.3 nm increases with temperature and product analysis experiments and time-resolved H atom detection by resonance fluorescence confirmed that high-temperature photolysis occurs.⁴¹ The fitted yields of molecular methane showed no dependence on $[\text{C}_2\text{H}_4]$, with $R_{\text{CH}_4}^0 = 2.0 \pm 0.46$. Correcting for the hydrogen atom yield produced via the photolysis of methyl radicals at 46 mJ gives $R_{\text{H}} = 3.62 \pm 0.31$.

As a further check on the values of R_{H} and $R_{\text{CH}_4}^0$ obtained from the scavenging experiments, the dependence of R_{CH_4} on I and pressure was simulated. The removal of hydrogen atoms at the cell walls was included in the simulations; its rate was calculated as described earlier, with a wall loss efficiency of 0.5, which was found necessary to bring the 300 K simulated and experimental methane yields into agreement at all pressures (Table IV). The results of the simulations are shown together with the experimental values of R_{CH_4} at in Figure 5b. The experimental upturn in R_{CH_4} at low intensities is reproduced at both pressures, although the absolute experimental values are somewhat underestimated. Increasing k_{10} by a factor of 2 brings the predicted and experi-

TABLE V: Summary of Primary Processes Occurring in the ArF Photolysis of Acetone

	process	$\phi_{300\text{K}}^a$	$\phi_{600\text{K}}$
P1	$\text{CH}_3 + \text{CO} + \text{CH}_3$	0.954	0.942
P2	$\text{H} + \text{CH}_2\text{COCH}_3$	0.028	0.033
P3	$\text{CH}_4 + \text{CH}_2\text{CO}$	0.015	0.018
P4	minor channels	0.003	0.007

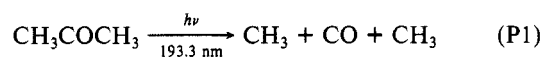
^a ϕ 's are normalized to unity and do not represent absolute quantum yields.

mental values into good agreement; given the uncertainty in this indirectly measured rate constant, a change of a factor or two is not unreasonable. Alternatively, an increase in R_{CH_4} would result, if some thermal decomposition of the acetonyl radical occurred at 600 K.

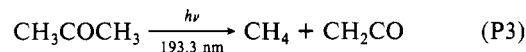
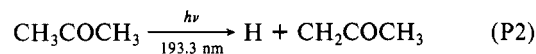
The experimental behavior at 600 K is thus consistent with the photolysis mechanism proposed to explain the results at room temperature, if the reactions of hydrogen atoms and methyl radicals with the precursor are allowed for.

Summary

Under all conditions employed in the present study, by far the most important channel in the 193.3-nm photolysis of acetone is that producing methyl radicals and carbon monoxide



Methyl radicals accounted for more than 95% of the radical products of the photolysis. At least four other primary dissociative processes were identified, of which the most important are



Photolysis channels P1–P3 account for >99% of the observed photolysis products under all conditions. The yields ϕ_i at 300 and 600 K for the identified primary processes, normalized to unity, are summarized in Table V. It is emphasized that the ϕ_i are not quantum yields but are calculated from the fractional yields of the observed products.

Although no significant pressure dependence of ϕ_1 or ϕ_4 was observed, ϕ_2 and ϕ_3 were obtained from data at the highest pressure employed at each temperature. As the yield of (P1) is much greater than the yields of all the other channels, changes in ϕ_2 and ϕ_3 with pressure would not noticeably affect ϕ_1 ; it is therefore possible that ϕ_2 and particularly ϕ_3 are somewhat dependent on pressure.

In addition to the primary, single-photon channels, a minor secondary photolysis process, involving the absorption of a second 193.3-nm photon by vibrationally excited methyl radicals, produced via (P1), was also observed.



The fraction of methyl radicals photolyzed in this way depends linearly on laser intensity, with $([\text{CH}_2]/[\text{CH}_3])_{t=0}$ given by $(0.31 \pm 0.21)F$ at 300 K and $(0.48 \pm 0.19)F$ at 600 K, where F is the fractional photolysis of the precursor per laser pulse.

In conclusion, the photolysis of acetone at 193.3 nm has been shown to provide an extremely clean source of methyl radicals, suitable for use in high-temperature studies of methyl radical reaction rates. As a result of the present study, acetone has been successfully used as a methyl radical source to study methyl radical recombination at temperatures up to 900 K.³⁵ Calculations of the rates of chain-mediated decomposition of acetone and of H abstraction of CH_3 from acetone demonstrate that, even at 900 K, there is a negligible perturbation of the recombination mechanism under typical experimental conditions.³⁵

Registry No. CH_3COCH_3 , 67-64-1; CH_3 , 2229-07-4; CO , 630-08-0; H , 12385-13-6; CH_2COCH_3 , 3122-07-4; CH_4 , 74-82-8; CH_2CO , 463-51-4; CH_2 , 2465-56-7; ethane, 74-84-0.

(41) Brouard, M.; Lightfoot, P. D.; Pilling, M. J. *J. Phys. Chem.* **1986**, *90*, 445.